HHS Public Access

Author manuscript

Biomaterials. Author manuscript; available in PMC 2016 June 01.

Published in final edited form as:

Biomaterials. 2015 June ; 52: 71–78. doi:10.1016/j.biomaterials.2015.01.079.

Self-Assembling Multidomain Peptides Tailor Biological Responses through Biphasic Release

Vivek A. Kumar[1], **Nichole L. Taylor**[1], **Siyu Shi**[1], **Navindee C. Wickremasinghe**[1], **Rena N. D'Souza**[2], and **Jeffrey D. Hartgerink**[1,*]

[1]Department of Chemistry, Department of Bioengineering, Rice University, Houston, TX 77030

[2]School of Dentistry, University of Utah, Salt Lake City, UT 84112

Abstract

Delivery of small molecules and drugs to tissues is a mainstay of several tissue engineering strategies. Next generation treatments focused on localized drug delivery offer a more effective means in dealing with refractory healing when compared to systemic approaches. Here we describe a novel multidomain peptide hydrogel that capitalizes on synthetic peptide chemistry, supramolecular self-assembly and cytokine delivery to tailor biological responses. This material is biomimetic, shows shear stress recovery and offers a nanofibrous matrix that sequesters cytokines. The biphasic pattern of cytokine release results in the spatio-temporal activation of THP-1 monocytes and macrophages. Furthermore, macrophage-material interactions are promoted without generation of a proinflammatory environment. Subcutaneous implantation of injectable scaffolds showed a marked increase in macrophage infiltration and polarization dictated by cytokine loading as early as 3 days, with complete scaffold resorption by day 14. Macrophage interaction and response to the peptide composite facilitated the (i) recruitment of monocytes/macrophages, (ii) sustained residence of immune cells until degradation, and (iii) promotion of a pro-resolution M2 environment. Our results suggest the potential use of this injectable cytokine loaded hydrogel scaffold in a variety of tissue engineering applications.

Keywords

Self-assembly; multi-domain peptide; inflammation; macrophage polarization

*Address correspondence to: Prof. Jeffrey D. Hartgerink, Department of Chemistry, Department of Bioengineering, Rice University, Mail Stop 602, 6100 Main St, Houston, TX 77030, Tel: (713) 348-4142, jdh@rice.edu.

The authors have no conflicts of interest to declare.

Supporting Information

Demonstration of stable in vitro THP-1 macrophage polarization due to addition of cytokines (Figure S1), and macrophage polarization as a function of release of cytokines from hydrogels (Supplemental Figure 2). Chemotaxis of THP-1 cells as a function of scaffold loading (Figure S3). Enlarged images of immunostained macrophages in vitro and in vivo (Figure S4–S14).

Introduction

Tissue engineering employs several strategies for the design and delivery of small molecules, drugs, chemokines and cytokines [1–3]. Multidomain peptides (MDP) designed by our lab self-assemble into β-sheets that further form entangled fibrous meshes. These highly hydrated meshes have been shown to generate nanofibrous hydrogels that can be tuned to promote cell adhesion and proliferation [4]. Capitalizing on this, we have designed MDP carriers that allow for release of growth factors for augmented in vitro and in vivo tissue responses [5–7]. In this study we utilize these self-assembling peptides for controlled spatio-temporal cytokine and chemokine release that augment immune responses in vitro and in vivo [6, 8, 9].

At the cellular level, circulating monocytes and tissue macrophages are intimately involved in modulating the immune response [10, 11]. Activation of resident cells (monocytes, macrophages and dendritic cells) result in the secretion of proinflammatory cytokines including TNF-α, IL-1β, IL-6, IL-23, and chemokines such as MCP-1 [10–12]. Monocyte chemoattractant protein-1, MCP-1 (CCL-2), is important for the recruitment of naïve monocytes to the injury site. These monocytes help in the clearance of the pro-inflammatory stimuli by production of reactive oxygen/nitrogen species (ROS/RNS), phagocytosis, and an adaptive immune response with B and T cells [13–15]. In normal resolution of inflammation, resident lineage committed pro-inflammatory M1 macrophages, and newly recruited naïve M0 macrophages exhibit plasticity towards an M2 pro-healing/anti-inflammatory phenotype. Macrophage plasticity is dependent on the extracellular milieu which is influenced by pathogens, extracellular matrix cues and mesenchymal cells, immune cells, tissue specific cells and cytokines/chemokines [12]. Several cytokines are known to influence a pro-resolution phenotype, including IL-10, IL-13, and IL-4. IL-4 specifically has been shown to encourage M1 cells to re-enter the cell cycle towards M2, decrease M1 activation and to induce M2 cell proliferation in-situ. IL-4 induced secretion of IL-10, IL-4, PDGF and TGF-β results in an amplification of the M2 response and the promotion of wound/tissue healing [16–19].

We hypothesize that a temporally controlled concert of cytokines to recruit (MCP-1) and differentiate (IL-4) naïve and tissue resident macrophages, can potentially modulate the in vitro response to cytokine/chemokine releasing scaffolds. Utilizing drug release modeling, human cell phenotype modulation, and in vivo macrophage polarization, we demonstrate the potential for this advanced functional material in tissue engineering applications.

Materials and Methods

MDP design and characterization

Multidomain peptides were designed based on previously published sequences from our laboratory: SL: $K_2(SL)_6K_2$ and SLac: $K(SL)_2(SLRG)(SL)_3K(GRGDS)$ [6]. All peptides, resin and coupling reagents were purchased from Aapptec (Louisville, KY). Standard solid phase peptide synthesis was performed on an Apex Focus XC (Aapptec), using Rink amide resin with 0.37mM loading and N-terminal acetylation. Post cleavage from resin, peptides were dialyzed with 500–1200 MWCO dialysis tubing (Sigma-Aldrich, St. Louis, MO)

against DI water. Peptides were subsequently lyophilized, confirmed for purity using electron-spray ionization mass spectrometry, MicroTOF ESI (Bruker Instruments, Billerica, MA), and reconstituted at 20 mg/mL in sterile 298 mM sucrose. Gelation of peptide was achieved by addition of volume equivalents of pH 7.4 buffer with 1X PBS or HBSS. For certain studies comparison to biosynthetic scaffolds was performed. Scaffolds used include: acid solubilized Type I rat tail tendon collagen (4.0 mg/mL neutralized), Matrigel™ (8.2 mg/mL) and tissue culture polystyrene (TCP) which were all obtained from BD Biosciences (Franklin Lakes, NJ).

Drug loading and release

MCP-1 or IL-4 (R&D Systems, Minneapolis, MN) was dissolved in HBSS and loaded into 200 μL of hydrogel (100 μL of SLac dissolved in 298mM surcose + 100 μL of cytokine) in the basolateral chamber of 24 well plates with 8.0 μm inserts. 1 mL of release media (HBSS) was added to the basolateral chamber, 400 μL to the apical chamber. 100μL aliquots of release media were assayed from the apical chamber, with replenishment, at 1, 2, 4, 8 hr, 24, 48, 72 and 144 hr. For long term IL-4 release, aliquots were taken at 1, 2, 3, 6, 10, 16 and 24 days. Mass release of cytokine was determined using ELISAs specific for MCP-1 and IL-4 (R&D Systems), n=4 for 3 independent repeats. Data were plotted as a function of cumulative release of cytokine in Sigmaplot (Systat, Chicago, IL) and modeled. IL-4 release was modeled using the Korsmeyer-Peppas equation and MCP-1 release was modeled using an exponential function. First derivative of cumulative release curves were used to model release rate.

Monocyte/macrophage culture and differentiation

Human monocytic leukemia cell line, THP-1 cells (ATCC, Manassas, VA), were cultured in media (ATCC-formulated RPMI-1640 Medium supplemented + 0.05 mM 2-mercaptoethanol + fetal bovine serum (10%). 100mg/ml penicillin, and 100mg/ml streptomycin) at a concentration of 200,000 cells/mL. Cells were grown in suspension and diluted when concentration reached 0.8–1.0 million cells/mL. Media was changed every 3 days. THP-1 monocytes were cultured to M0 macrophages by pulsing with 5 nm phorbol 12-myristate 13-acetate, PMA (Sigma-Aldrich) for 5 mins. Adherent M0 differentiated cells were incubated with IFN-γ (20 ng/mL) (Gibco, Life Technologies, Carlsbad, CA) + LPS (20 ng/mL) (Sigma-Aldrich) for M1 phenotype or IL-4 (20 ng/mL) (R&D Systems) for 24 hours at 37°C. For macrophage plasticity studies, THP-1 cells were differentiated to M1 macrophages for 24 hr and then treated with experimental group.

Macrophage characterization

PCR and fluorescent immunostaining was used to characterize macrophage phenotype, n=4 for 3 independent repeats. PCR: RNA extraction was performed as per manufacturer's protocol (RNeasy, Qiagen, Gaithersburg, MD). RNA concentrations was determined using Nanodrop (Thermo Scientific, Waltham, MA), and reverse transcription to cDNA was performed using iScript (Qiagen), followed by RT-PCR using a Biorad 7300 (Biorad, Berkeley, CA) and SsoAdvanced SYBR-green KIT (Qiagen). PCR primers were purchased from Invitrogen. For M1 phenotype IL-1 (forward primer: GCTTGGTGATGTCTGGTCCAT, reverse primer: CACCACTTGTTGCTCCATATCCT)

[20] and M2 phenotype CD-36 (forward primer: TCACTGCGACATGATTAATGGTACA, reverse primer: ACGTCGGATTCAAATACAGCATAGAT) was used [21]. Amplification of the genes of interest was normalized to the amplification of L37-a (forward primer: ATTGAAATCAGCCAGCACGC, reverse primer: AGGAACCACAGTGCCAGATCC), a housekeeping gene constitutively expressed by macrophage phenotypes [21]. CT values were generated by the software were compared to L37-a expression. Expression of gene of interest was normalized to control expression noted in each experiment. Fluorescent immunostaining of cell surface markers of macrophage phenotype was performed for CD68 (pan-macrophage), IL-1r (M1), CD36 (M2) and CD206 (M2), (BioLegend, San Diego, CA).

Immunomodulation of macrophage phenotype due to drug releasing gels

Hydrogels were loaded with either MCP-1, IL-4, or combo gel (MCP-1 + IL-4) at a concentration of 1 μg/mL each in HBSS. 200 μL of the MDP + 200μL of cytokine mixture was loaded into each well (n=4 for 3 independent repeats). 1 mL of media was added on top of the gels. Controls were made by adding cytokines known to induce the desired macrophage differentiation to media at a concentration of 20 ng/mL: M1 control (LPS and IFN-γ), M2 control (IL-4), and M0 control (no cytokine). THP-1 monocytes were pulsed with (PMA), washed, resuspended in media, seeded at 500,000 cells in 400 μL media, per 0.4 μm transwell inserts (24 well) and incubated for 16 hr, 37°C. To determine cytokine release influencing macrophage plasticity, THP-1 cells were differentiated to M1 macrophages in inserts for 24 hr and then treated with IL-4 containing gels. Differentiated cells were probed for phenotype by RNA extraction and PCR; or in situ fixation and immunofluorescence staining (detailed above).

Cytokine dependent chemotaxis

Chemotaxis due to cytokine release from hydrogels was measured using a transwell set up. THP-1 cells were seeded in 8.0 μm transwell inserts at a density of 200,000 cells/insert in media in the apical chamber. Drug eluting hydrogels were loaded with 0.1, 0.01, 0.001μg MCP-1 or IL-4 were loaded in the basolateral chamber. Media only wells served as negative control and media ± equivalent MCP-1/IL-4 concentration served as positive controls. The set up was incubated for 16 hr at 37°C. Cells in the transwell insert facing the apical side were wiped off with a cotton tipped applicator, and migrated cells on the insert were fixed with neutral buffered formalin for 15 mins, washed with PBS, and stained with crystal violet (0.2w% in 20% methanol-PBS) for 30 mins [22]. Migrating cells were counted in 6 random fields per sample (n=4 for 3 independent repeats).

Direct contact THP-1 cell-material interaction

200μL MDP gels were cast in 24 well plates. Collagen and Matrigel were used as gel controls, and TCP with macrophages differentiated to M1 (20ng/mL IFN-γ+LPS) and M2 (20 ng/mL IL-4) phenotype were used as cell controls. THP-1 cells in suspension were suspended in media and incubated at a concentration of 1M cells/well atop scaffolds. Media aliquots were assayed for inflammatory (IL-1β, TNF-α), and anti-inflammatory (IL-10) at 24 hr using ELISA (Biolegend, CA). Cells on scaffolds were fixed with formalin and cellular actin was stained with AlexaFluor® 488 Phalloidin and nuclei with DAPI (Invitrogen). Cells on scaffolds were imaged using confocal microscopy (Nikon A-1 RSI confocal microscope,

Tokyo, Japan) to note surface coverage and gel infiltration. DAPI stained cell nuclei were counted from 6 random fields per replicate using NIH ImageJ (n=4 for 3 independent repeats). To image cell-nanofiber interactions, THP-1 cells on SLac scaffolds were fixed in formalin, ethanol dehydrated in a graded series (30%, 50%, 75%, 90%, 95%, 100% twice) and critical point dried, sputter coated with 7 nm gold (Denton, Moorestown, NJ), and imaged using scanning electron microscopy (SEM) on a FEI Quanta 400 ESEM (FEI Company, Hillsboro, OR). A subset of SEM images were false colored using Adobe Photoshop® (Adobe Systems, San Jose, CA) to delineate cells on scaffolds.

Endotoxin testing

To determine macrophage activation due to LPS load of materials, 200 μL gels were cast and incubated with 200 μL PBS for 24 hr. PBS was assayed for endotoxin content and normalized per unit mass of material, Pierce LAL Chromogenic Endotoxin Quantitation Kit (Thermo Scientific, Rockford, IL), n=4 for 3 independent experiments.

Subcutaneous implants

All experiments were approved by the Rice University Institutional Animal Care and Use committee. Female Wisar rats (225–250g, Charles River Labs, Wilmington, MA) were anesthetized using isofluorane (2% for induction and 1% for maintenance), dorsal aspect shaved and sterilely prepped. Scaffolds were loaded in syringes and 200μL subcutaneous injections of each SLac, SLac+MCP-1, SLac+IL-4, and SLac+MCP-1+IL-4 were made in 4 different 1.5 inch spaced randomized sites on the dorsal aspect, on either side between the lower thoracic and upper lumber vertebrae, n=4 for each scaffolds, for each timepoint. At prescribed timepoints 3 day, 1 week, and 2 weeks rats were euthanized using an overdose of isoflurane, CO_2 asphyxiation, and bilateral thoracic puncture. The dorsal skin was removed around the entire implant, washed with PBS, and fixed in neutral buffered formalin for 24 hr prior to processing. Tissue was then processed into paraffin blocks, sectioned at 7μm, deparraffinized and stained for cellular infiltrate using hematoxylin and eosin (H&E), and nuclei in 3 random fields per sample and averaged over all samples from each group were counted using ImageJ (NIH, Bethesda, MD). Infiltration of implants was graded on a 5 point scale: 1: periphery (<50%, with large parts of scaffold uninfiltrated, center uninfiltrated); 2: 50–80% (with small regions of scaffold exposed, center uninfiltrated); 3: center infiltrated (with small regions of scaffold exposed); 4: few to no scaffold regions visible; 5: implant indistinguishable from native tissue except for complete dense cellular repopulation. Cellular infiltrate was phenotyped using immunostaining. Immune cell staining was performed for 1) pan-macrophage rabbit anti-rat CD68 (Abcam), M1 macrophages goat anti-rat CCR7 (Novus), M2 macrophages mouse anti-rat CD163 (AbDSerotec). Secondary antibodies used were: 1) AF647 donkey anti-rabbit, 2) AF488 donkey anti-goat, 3) AF555-donkey anti-mouse (Life Technologies). Nuclei were counterstained with DAPI (Life Technologies). Cellular infiltrate was quantified using NIH Image J and M1/M2 polarization ratio was determined.

Statistical analysis

Data is represented as Mean ± S.D. Differences between paired data were compared using Student’s t-test, and ANOVA with Tukey post hoc analysis for multiple comparisons of

parametric data and Kruskal-Wallis ANOVA with Dunn's post hoc analysis for non-parametric data. Values of $p < 0.01$ were considered statistically significant.

Results

MDP scaffolds for tissue engineering

MDP scaffolds used in this study were composed of the sequence KSLSLSLRGSLSLSLKGRGDS (termed SLac). Self-assembling nanofibers have been evaluated using ATR-FTIR and AFM demonstrating the anti-parallel stacking of peptides into fibrillar ribbons (6 nm wide x 2 nm tall) [9]. After addition of polyvalent anions (eg. PO_4^{3-}) in buffer, terminal lysine residues form ionic interactions with PO_4^{3-} groups crosslinking the matrix into a hydrogel with interconnected pores (Figure 1). These pores, coupled with the nanofibers, act as a physical barrier and increase tortuosity for drug delivery. Given the reversible nature of bonds that partake in self-assembly, hydrogels exhibit shear thinning and recovery [8]. This allows easy syringe aspiration and delivery locally or via catheter, demonstrated previously in a LPS-renal toxicity kidney rescue model [23]. Here we have loaded SLac with cytokines and demonstrate a biphasic drug delivery platform without the addition of exogenous carrier molecules or dopants [24].

Cytokine/Chemokine release

MCP-1 was chosen due to its robust chemoattractant potential. Equal volumes of MCP-1 dissolved in HBSS was mixed with 2 w% SLac. The final 1 w% gel released MCP-1 at approximately the same normalized rate regardless of initial loading amount (1–100ng/200μL of gel). Up to 80% release was achieved over the first 48 hr, similar to previous studies using MCP-1 [13, 22] (Figure 2 A–C).

IL-4 was loaded in a similar manner into hydrogels. IL-4's potent M2 stimulating activity has been widely reported and thus justified its use [10, 11, 25, 26]. Loading and release studies were performed similar to MCP-1. Similar to MCP-1, cytokine loading concentration did not impact normalized release profiles. In contrast to MCP-1 release however, IL-4 exhibited prolonged release over 16 days (Figure 2D–G).

MCP-1 release rate was modeled using an exponential decay Weibull function (R^2>0.95), (Figure 1C), such that the first derivative gave Equation 1:

$$\frac{dM_{MCP-1}}{dt} = 19.4 \times e^{-0.24t} \quad (1)$$

And IL-4 release was modeled using a Korsmeyer-Peppas function (R^2>0.95), (Figure 1C), such that the first derivate gave Equation 2:

$$\frac{dM_{IL-4}}{dt} = 0.87 \times t^{-0.49} \quad (2)$$

Both equations suggest diffusion based drug release (Figure 2H–I) [27, 28]. However, it appeared the higher IL-4 loading (100ng) resulted in more rapid diffusion, with a larger power term for the modeled diffusion equation, compared to lower loading concentrations (1 or 10ng loading), suggesting interaction of IL-4 molecules with the MDP matrix.

Potency of the released cytokines on monocytes/macrophages

The potential of our therapeutic strategy in humans was demonstrated with evolving proliferative THP-1 cells that dynamically challenge the therapeutic regimen presented to them [29]. Using PCR and immunofluorescence staining, stable in vitro differentiation of THP-1 cells into $CD68^{+}$ M0 macrophages, $CD68^{+}IL7r^{+}IL\text{-}1^{+}CD36^{-}CD206^{-}$ M1 macrophages and $CD68^{+}IL7r^{-}IL\text{-}1^{-}CD36^{+}CD206^{+}$ M2 macrophages based on addition of PMA (M0), IFN-γ and LPS (M1), and IL-4 (M2) was established (Figure S1) [29, 30]. Further, macrophage plasticity from predifferentiated, lineage committed M1 macrophages to M2 macrophages after the addition of IL-4 was shown (Figure S1). Repeating experiments in transwell inserts, with or without MDP hydrogels releasing MCP-1, IL-4 or MCP-1 + IL-4 helped elucidate the effect of cytokines on macrophage phenotype (Figure S2). MDP gels alone, MCP-1 in media or within gels had no pro- or anti-inflammatory effect on PMA differentiated THP-1 cells. However, addition of IL-4 to the media or any gels that were releasing IL-4 alone or in concert with MCP-1 resulted in a robust M2 response (Figure S2 F–J). Critically, we demonstrated plasticity of macrophages through phenotypic conversion of cells which were already M1 lineage committed to M2 (Figure S2 H–J). Together these data establish a routine method for the development of specific macrophage lineages, immunostaining of those lineages and PCR quantitation of markers of cellular phenotype, noting that differences were considered significant if $p<0.01$.

The efficacy of MCP-1 delivery was determined using chemotaxis of THP-1 cells [22]. Addition of MCP-1 loaded MDP scaffolds in the basolateral chamber of a transwell setup resulted in characteristic dose dependent migration of THP-1 monocytes through 8 μm membrane pores (Figure S3). As expected no significant chemotactic effect with IL-4 addition to media or MDP alone, over media-only controls was observed (Figure S3). Together these results suggest the ability to recruit cells towards the cytokine loaded scaffold.

Specific interaction of macrophages with materials is an established method to determine the proclivity for stimulation of pro-inflammatory pathways [31]. Specific cell-material responses using THP-1 cells were probed for pro-inflammatory markers. THP-1 cells were incubated on scaffolds without preactivation with PMA, simulating macrophages being recruited to the material in vivo. These non-adherent monocytes surprisingly showed excellent adhesion to scaffolds, similar to M1 control cells (Figure 3). For comparison, biologically derived matrices, collagen and Matrigel™, known to be highly cell adherent were used as controls and showed significantly fewer cells adherent compared to MDP matrices ($p<0.01$). Endotoxin load of MDP scaffolds was similar to commercially available scaffolds, and orders of magnitude lower than that used for M1 activation. Furthermore, canonical proinflammatory markers TNF-α and IL-1β levels were similar for MDP scaffolds compared to negative control (Figure 3).

In vivo evaluation of injectable scaffolds

No redness or swelling at the implant site, or altered gait/behavior of rats was noted over the course of the study. Cellularization was determined by immunostaining and quantification for cellular infiltrate, and macrophage polarization (Figure 4). Cellular infiltration, determined by counting nuclei from H&E stained images, showed a significant dependence on MCP-1 loading. Scaffolds with MCP-1 showed the greatest number of infiltrating cells and the greatest degree of infiltration at the early timepoint (3 day) compared to SLac alone or IL-4 loaded scaffolds ($p<0.01$, Figure 4). Comparatively, at the 7 day time point, all scaffolds showed infiltration throughout, and a significant increase in the number of infiltrating cells ($p<0.01$, Figure 4). Further by day 7, scaffolds loaded with IL-4, or MCP-1 and IL-4 showed several distinct bloods vessels with circulating red blood cells (Figure 4). Macrophage polarization was dependent on IL-4 loading with a greater M2 polarization ratio in SLac+IL-4 or SLac+MCP-1+IL-4 compared to SLac+MCP-1 or unloaded scaffolds ($p<0.01$, Figure 6). Loaded MCP-1 and IL-4 appears to release into the surrounding tissue, recruiting macrophages and polarizing them towards and M2 phenotype both within scaffolds and around scaffolds (Figure 4). By the 14 day time point, MDP scaffolds had biodegraded and/or resorbed. Together these results indicate that over a very short period of 3 days - 1 week cytokine loaded injectable scaffolds promote a strong MCP-1 dependent infiltration response and IL-4 promotes M2 macrophage polarization, creating an environment which is proangiogeneic, which then resolves without creating a chronic wound by 14 days.

Discussion

Multidomain peptide (MDP) nanofiber hydrogel materials for this study have been well characterized for their physical and chemical properties by our group [6, 8, 9]. We have evaluated their cytocompatibility and utility in in vivo applications [5, 23]. Herein, we report the ability to use these self-assembling peptides, tailored to contain an MMP degradation sequence and RGDS adhesion sequence, for cytokine delivery [6]. Control of in vivo environments is critical to the success of implanted materials. To tailor in vivo responses, we utilized MCP-1 and IL-4 in this study. Unique to this materials/chemokine combination, we noted attenuated release of loaded cytokines. For example, unlike previous studies which employed microcarrier particles (eg. PLGA) [13] or anchoring proteins, [22] MDP matrices composed of nanofibers contain pores small enough to attenuate MCP-1 release for similar 48 hr periods. Prolonged IL-4 release from hydrogels may be useful to promote a M2/Th-2 response over 1–2 weeks, which would optimally match classically activated macrophage innate immune response [32]. Of note is that about 80% (MCP-1) and 40% (IL-4) of the cytokine loaded into gels was recovered. Loss of cytokine may be due to permanent entrapment of cytokine within gels, loss of detectable (ELISA) activity over the assay period due to degradation, or other mechanisms. To understand the differences in release profiles of MCP-1 and IL-4, release from scaffolds was modeled. To better elucidate the differences in release rate, the hydrodynamic volume and mass were determined from the amino acid sequence (www.basic.northwestern.edu/biotools/proteincalc.html). MCP-1 has a smaller mass (7.6 kDa) and hydrodynamic volume (9.14 nm^3) compared to IL-4 which is heavier (14.0 kDa) and larger (16.9 nm^3). The charge at neutral pH of MCP-1 is +5 compared to

+7.9 for IL-4. These distinct differences in molecular weight and hydrodynamic volume may play key factors in determining diffusivity of large charged molecules in a tortuous nanofibrillar hydrogel. Enhanced by potential interactions with the MDP matrix and charge stabilization, these factors suggest a mechanism for the prolonged release of IL-4 compared to MCP-1. However these differences are modest and other mechanisms may be in play [9, 33, 34]. Notwithstanding this incomplete understanding of the interaction of the cytokines with the MDP matrix, biphasic drug delivery of 2 cytokines in their therapeutically desired timeframes was observed (Figure 2). Complementing the design of our drug delivery system, we postulated that lineage uncommitted monocytes would be recruited to sites of inflammation acutely by delivery of MCP-1 over a 48 hr period, while sustained delivery of IL-4 over a 14–16 day period would enhance a long-term M2 micro-environment. In summary, the ability to modulate the inflammatory environment of both uncommitted and M1 lineage committed THP-1 cells towards an M2 phenotype has been demonstrated.

In addition to demonstrating in vitro chemotaxis and modulation of THP-1 cell phenotype, we noted that a marker of macrophage activation is development and spreading of filapodia, with concomitant actin filament polymerization. Phalloidin staining of actin filaments showed spread cells on SLac scaffolds with or without cytokines. SL scaffolds which do not contain the cell adhesion sequence showed significantly lower cell adhesion (further distinction between peptides are presented in the Materials and Methods). One common concern is that activation of THP-1 cells to an adherent phenotype is due to LPS from bacterial contamination. However, due to the chemical synthesis of these materials, this was not likely. Nevertheless, the endotoxin load of MDP scaffolds was assayed and noted that it was similar to commercially purchased collagen or Matrigel™, and significantly lower than that used for M1 activation, with concomitant low levels of proinflammatory markers TNF-α and IL-1β.

While these in vitro studies yielded vital information on the effects of MDP, cytokine loading and release; all macrophage phenotypes have not been completely identified and classified in humans, and perhaps clonally unique M0, M1, M2 macrophages are purely academic pursuits [17, 35]. Macrophages exhibit a spectrum of activation and polarization, exhibiting some subset of common markers either in high or low abundance. In the design of our study, a cell type that has been well reported to exhibit different aspects of this spectrum was chosen [21, 29]. THP-1 cells are a well studied/accepted monocytic leukemia cell line [21]. While it may be instructive to use a variety of other monocytes and macrophage cell types, including peripheral blood mononuclear cells, peritoneal lavaged monocytes, gut derived, bone marrow aspirate derived, liver derived or monocytes/macrophages from alternative species, we wanted to challenge our model with a cell line that is relatively homogeneous and that is well studied in the field [25, 30, 36, 37]. Further, since this study is specifically interested in the human cytokine-macrophage interaction, which is often species unique, human cells were chosen [25]. To overcome the inherent limitations of in vitro studies, we next exploited MDP shear thinning and rapid self-assembly [6, 8] to probe the effects of the scaffold and its constituents' release in a minimally invasive rat subcutaneous in vivo model.

In this subcutaneous in vivo model, we noted the ability for cells to infiltrate all hydrogel scaffolds without the need for a canonical macroporous structure. We hypothesize that (i) mimicry of the nanofibrous ECM structure, (ii) the RGD binding moiety, (iii) MMP cleavage site, and (iv) facile breaking and reforming of hydrophobic and ionic interactions, promote host cell infiltration of the engineered scaffolds without the formation of a fibrous capsule walling off the implant [5, 6, 8]. Simultaneously the loaded nanofibrous hydrogel tailors the cytokine mediated foreign body response by influencing the cellular phenotype within scaffolds and in the vicinity of scaffolds [32, 35, 38, 39]. Capitalizing on chemical functionality, our group and others have demonstrated in recent studies strategies using self-assembling peptide materials to modulate in vivo phenotype to tailor adjuvant responses [40], act as DNA nanovectors, and provide distinct moieties for angiogenesis and tissue regeneration [34, 41]. In summary, the minimally invasive injectable self-assembling SLac hydrogel implant in the rat subcutaneous space has helped elucidate the host response to cytokine loaded compositions, without concomitant physiologic or pathophysiologic factors/contaminants present in disease models.

Conclusion

The data presented in this study outline the development of a platform for sequential, biphasic drug delivery of 2 key cytokines in directing the biological response in vitro and in vivo. Through control of molecular self-assembly, shear thinning and shear recovering MDP can be injected in situ via needle. MDP scaffolds can deliver MCP-1 acutely to recruit naïve monocytes to the region of inflammation and deliver IL-4 over a prolonged period that is characteristic of the acute immune response. Our minimally invasive in vivo model demonstrated cytokine dependent infiltration and development of M2 macrophage phenotype, without creation of a chronic wound. We envision the use of these hybrid materials in a host of tissue engineering applications.

Supplementary Material

Refer to Web version on PubMed Central for supplementary material.

Acknowledgments

The work presented in this manuscript was support by grants from the NIH for J.D.H. (R01 DE021798) and V.A.K. (F32 DE023696).

References

1. Langer R, Vacanti JP. Tissue engineering. Science. 1993; 260:920–926. [PubMed: 8493529]
2. Langer R, Tirrell DA. Designing materials for biology and medicine. Nature. 2004; 428:487–492. [PubMed: 15057821]
3. Lee KY, Peters MC, Anderson KW, Mooney DJ. Controlled growth factor release from synthetic extracellular matrices. Nature. 2000; 408:998–1000. [PubMed: 11140690]
4. Kang MK, Colombo JS, D'Souza RN, Hartgerink JD. Sequence Effects of Self-Assembling MultiDomain Peptide Hydrogels on Encapsulated SHED Cells. Biomacromolecules. 2014; 15:2004–2011. [PubMed: 24813237]

5. Galler KM, Hartgerink JD, Cavender AC, Schmalz G, D'Souza RN. A customized self-assembling peptide hydrogel for dental pulp tissue engineering. Tissue Eng Part A. 2012; 18:176–184. [PubMed: 21827280]
6. Galler KM, Aulisa L, Regan KR, D'Souza RN, Hartgerink JD. Self-assembling multidomain peptide hydrogels: designed susceptibility to enzymatic cleavage allows enhanced cell migration and spreading. J Am Chem Soc. 2010; 132:3217–3223. [PubMed: 20158218]
7. Galler KM, Cavender A, Yuwono V, Dong H, Shi S, Schmalz G, et al. Self-assembling peptide amphiphile nanofibers as a scaffold for dental stem cells. Tissue Eng Part A. 2008; 14:2051–2058. [PubMed: 18636949]
8. Bakota EL, Wang Y, Danesh FR, Hartgerink JD. Injectable multidomain peptide nanofiber hydrogel as a delivery agent for stem cell secretome. Biomacromolecules. 2011; 12:1651–1657. [PubMed: 21417437]
9. Dong H, Paramonov SE, Aulisa L, Bakota EL, Hartgerink JD. Self-assembly of multidomain peptides: balancing molecular frustration controls conformation and nanostructure. J Am Chem Soc. 2007; 129:12468–12472. [PubMed: 17894489]
10. Wynn TA, Chawla A, Pollard JW. Macrophage biology in development, homeostasis and disease. Nature. 2013; 496:445–455. [PubMed: 23619691]
11. Buckley CD, Gilroy DW, Serhan CN, Stockinger B, Tak PP. The resolution of inflammation. Nat Rev Immunol. 2013; 13:59–66. [PubMed: 23197111]
12. Laskin DL. Macrophages and inflammatory mediators in chemical toxicity: a battle of forces. Chem Res Toxicol. 2009; 22:1376–1385. [PubMed: 19645497]
13. Roh JD, Sawh-Martinez R, Brennan MP, Jay SM, Devine L, Rao DA, et al. Tissue-engineered vascular grafts transform into mature blood vessels via an inflammation-mediated process of vascular remodeling. Proc Natl Acad Sci U S A. 2010; 107:4669–4674. [PubMed: 20207947]
14. Low QE, Drugea IA, Duffner LA, Quinn DG, Cook DN, Rollins BJ, et al. Wound healing in MIP-1alpha(−/−) and MCP-1(−/−) mice. Am J Pathol. 2001; 159:457–463. [PubMed: 11485904]
15. DiPietro LA, Burdick M, Low QE, Kunkel SL, Strieter RM. MIP-1alpha as a critical macrophage chemoattractant in murine wound repair. J Clin Invest. 1998; 101:1693–1698. [PubMed: 9541500]
16. Murray PJ, Wynn TA. Protective and pathogenic functions of macrophage subsets. Nat Rev Immunol. 2011; 11:723–737. [PubMed: 21997792]
17. Mosser DM, Edwards JP. Exploring the full spectrum of macrophage activation. Nat Rev Immunol. 2008; 8:958–969. [PubMed: 19029990]
18. Kharraz Y, Guerra J, Mann CJ, Serrano AL, Munoz-Canoves P. Macrophage plasticity and the role of inflammation in skeletal muscle repair. Mediators Inflamm. 2013; 2013:491497. [PubMed: 23509419]
19. Freytes DO, Kang JW, Marcos-Campos I, Vunjak-Novakovic G. Macrophages modulate the viability and growth of human mesenchymal stem cells. J Cell Biochem. 2013; 114:220–229. [PubMed: 22903635]
20. Spencer M, Yao-Borengasser A, Unal R, Rasouli N, Gurley CM, Zhu B, et al. Adipose tissue macrophages in insulin-resistant subjects are associated with collagen VI and fibrosis and demonstrate alternative activation. Am J Physiol Endocrinol Metab. 2010; 299:E1016–1027. [PubMed: 20841504]
21. Maess MB, Sendelbach S, Lorkowski S. Selection of reliable reference genes during THP-1 monocyte differentiation into macrophages. BMC Mol Biol. 2010; 11:90. [PubMed: 21122122]
22. Lin CC, Boyer PD, Aimetti AA, Anseth KS. Regulating MCP-1 diffusion in affinity hydrogels for enhancing immuno-isolation. J Control Release. 2010; 142:384–391. [PubMed: 19951731]
23. Wang Y, Bakota E, Chang BH, Entman M, Hartgerink JD, Danesh FR. Peptide nanofibers preconditioned with stem cell secretome are renoprotective. J Am Soc Nephrol. 2011; 22:704–717. [PubMed: 21415151]
24. Yoo JW, Irvine DJ, Discher DE, Mitragotri S. Bio-inspired, bioengineered and biomimetic drug delivery carriers. Nat Rev Drug Discov. 2011; 10:521–535. [PubMed: 21720407]
25. Gordon S, Taylor PR. Monocyte and macrophage heterogeneity. Nat Rev Immunol. 2005; 5:953–964. [PubMed: 16322748]

26. Pollard JW. Trophic macrophages in development and disease. Nat Rev Immunol. 2009; 9:259–270. [PubMed: 19282852]
27. Siepmann J, Siepmann F. Modeling of diffusion controlled drug delivery. J Control Release. 2012; 161:351–362. [PubMed: 22019555]
28. Dash S, Murthy PN, Nath L, Chowdhury P. Kinetic modeling on drug release from controlled drug delivery systems. Acta Pol Pharm. 2010; 67:217–223. [PubMed: 20524422]
29. Daigneault M, Preston JA, Marriott HM, Whyte MK, Dockrell DH. The identification of markers of macrophage differentiation in PMA-stimulated THP-1 cells and monocyte-derived macrophages. PLoS One. 2010; 5:e8668. [PubMed: 20084270]
30. Tjiu JW, Chen JS, Shun CT, Lin SJ, Liao YH, Chu CY, et al. Tumor-associated macrophage-induced invasion and angiogenesis of human basal cell carcinoma cells by cyclooxygenase-2 induction. J Invest Dermatol. 2009; 129:1016–1025. [PubMed: 18843292]
31. Motlagh D, Yang J, Lui KY, Webb AR, Ameer GA. Hemocompatibility evaluation of poly(glycerol-sebacate) in vitro for vascular tissue engineering. Biomaterials. 2006; 27:4315–4324. [PubMed: 16675010]
32. Zhang L, Cao Z, Bai T, Carr L, Ella-Menye JR, Irvin C, et al. Zwitterionic hydrogels implanted in mice resist the foreign-body reaction. Nat Biotechnol. 2013; 31:553–556. [PubMed: 23666011]
33. Branco MC, Pochan DJ, Wagner NJ, Schneider JP. The effect of protein structure on their controlled release from an injectable peptide hydrogel. Biomaterials. 2010; 31:9527–9534. [PubMed: 20952055]
34. Wickremasinghe NC, Kumar VA, Hartgerink JD. Two-step self-assembly of liposome-multidomain peptide nanofiber hydrogel for time-controlled release. Biomacromolecules. 2014; 15:3587–3595. [PubMed: 25308335]
35. Spiller KL, Anfang RR, Spiller KJ, Ng J, Nakazawa KR, Daulton JW, et al. The role of macrophage phenotype in vascularization of tissue engineering scaffolds. Biomaterials. 2014; 35:4477–4488. [PubMed: 24589361]
36. Nahrendorf M, Swirski FK. Monocyte and macrophage heterogeneity in the heart. Circ Res. 2013; 112:1624–1633. [PubMed: 23743228]
37. Schneberger D, Aharonson-Raz K, Singh B. Monocyte and macrophage heterogeneity and Toll-like receptors in the lung. Cell Tissue Res. 2011; 343:97–106. [PubMed: 20824285]
38. Mokarram N, Bellamkonda RV. A perspective on immunomodulation and tissue repair. Ann Biomed Eng. 2014; 42:338–351. [PubMed: 24297492]
39. Mokarram N, Merchant A, Mukhatyar V, Patel G, Bellamkonda RV. Effect of modulating macrophage phenotype on peripheral nerve repair. Biomaterials. 2012; 33:8793–8801. [PubMed: 22979988]
40. Hudalla GA, Sun T, Gasiorowski JZ, Han H, Tian YF, Chong AS, et al. Gradated assembly of multiple proteins into supramolecular nanomaterials. Nat Mater. 2014; 13:829–836. [PubMed: 24930032]
41. Kumar VA, Taylor NL, Shi S, Wang BK, Jalan AA, Kang MK, et al. Highly Angiogenic Peptide Nanofibers. ACS Nano. 2015

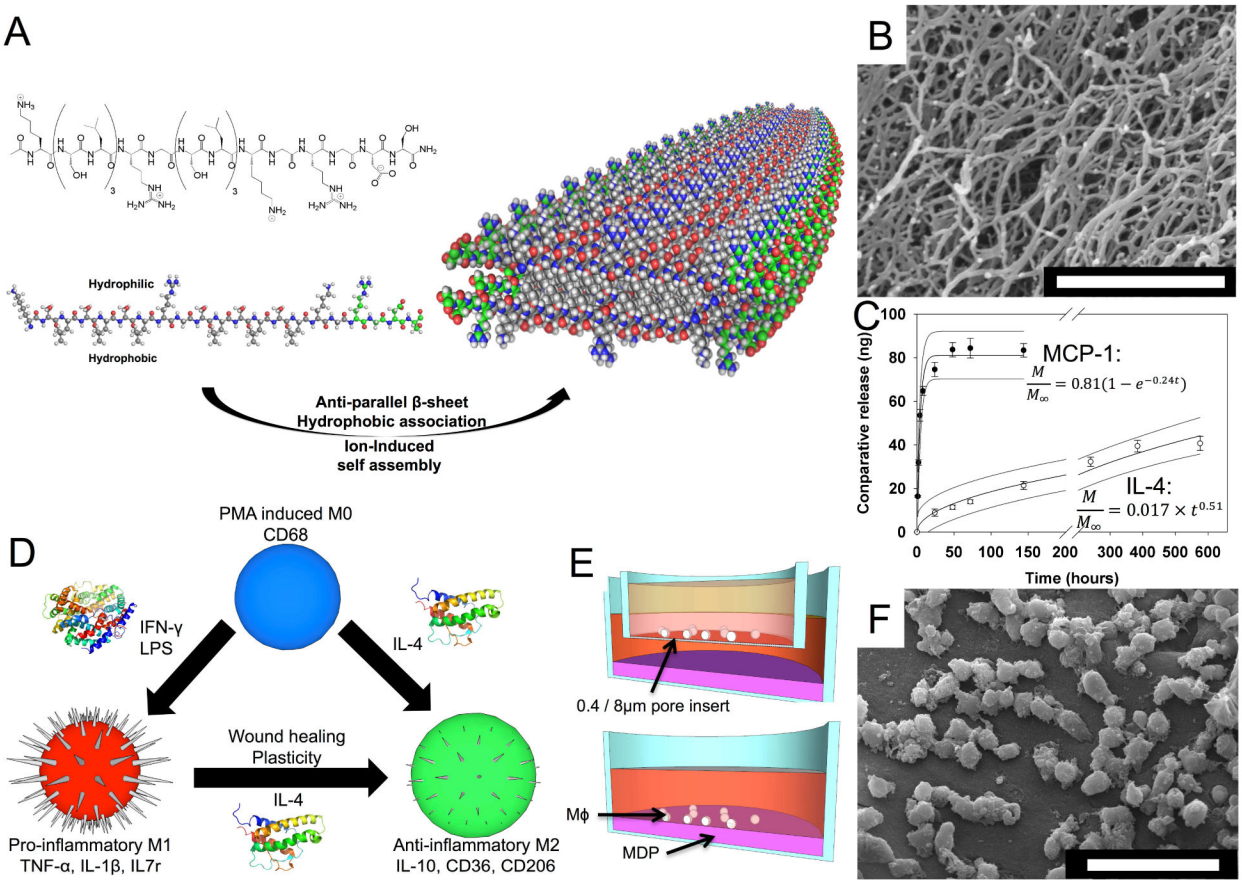

Figure 1. Design and immunologic evaluation of multidomain peptides

(A) $K(SL)_3RG(SL)_3KGRGDS$ "SLac" peptides undergo ion triggered self-assembly, to form large scale nanofibers (B). (C) Cytokine release was tailored for short term MCP-1 and long term IL-4 release and modeled as a function of time (R^2=0.98 for each). (D) THP-1 monocyte/macrophage phenotype was modulated using pro-inflammatory IFN-γ and LPS, or anti-inflammatory (IL-4). (E) Cell phenotype and chemotaxis as a function of cytokine was determine using a transwell set up, and cell-material interaction was probed by direct seeding (E and F). Scale bar (B): 1 μm, (F): 50 μm.

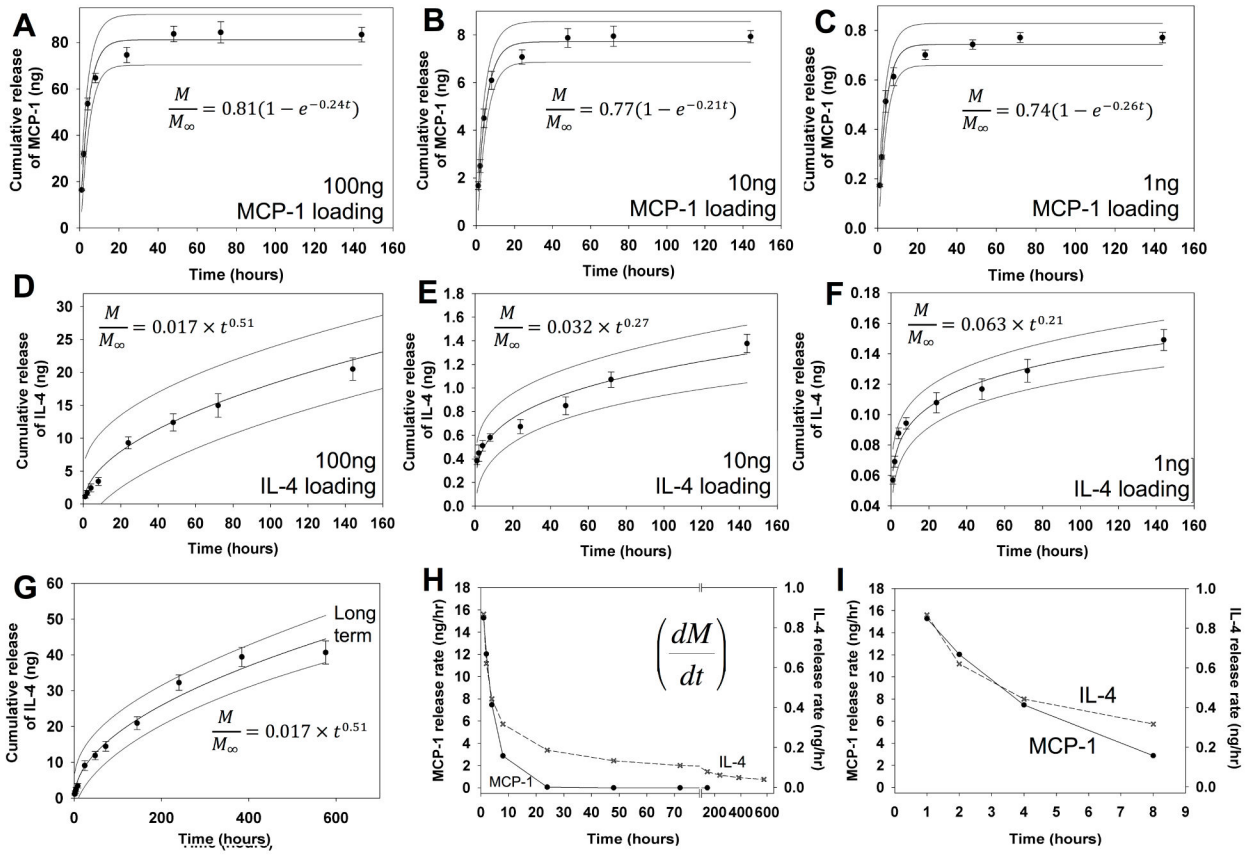

Figure 2. MCP-1 and IL-4 release from hydrogels

MCP-1 was loaded into hydrogels (A) 100 ng, (B) 10 ng and (C) 1 ng. Cumulative release curves indicate 80% of loaded cytokine is released over the first 48 hr. IL-4 was loaded into hydrogels at a concentration of (D) 100 ng, (E) 10 ng and (F) 1 ng. Cumulative release curves indicate about 15–20% of loaded cytokine is released over the first 6 days, with up to 40% release after 16 days (G). Release rate was plotted as the first derivative of cumulative release rate (H), with the first 8 hours shown in detail (I). Release was modeled, best fit curve and with 95% CI bands for A–G are shown.

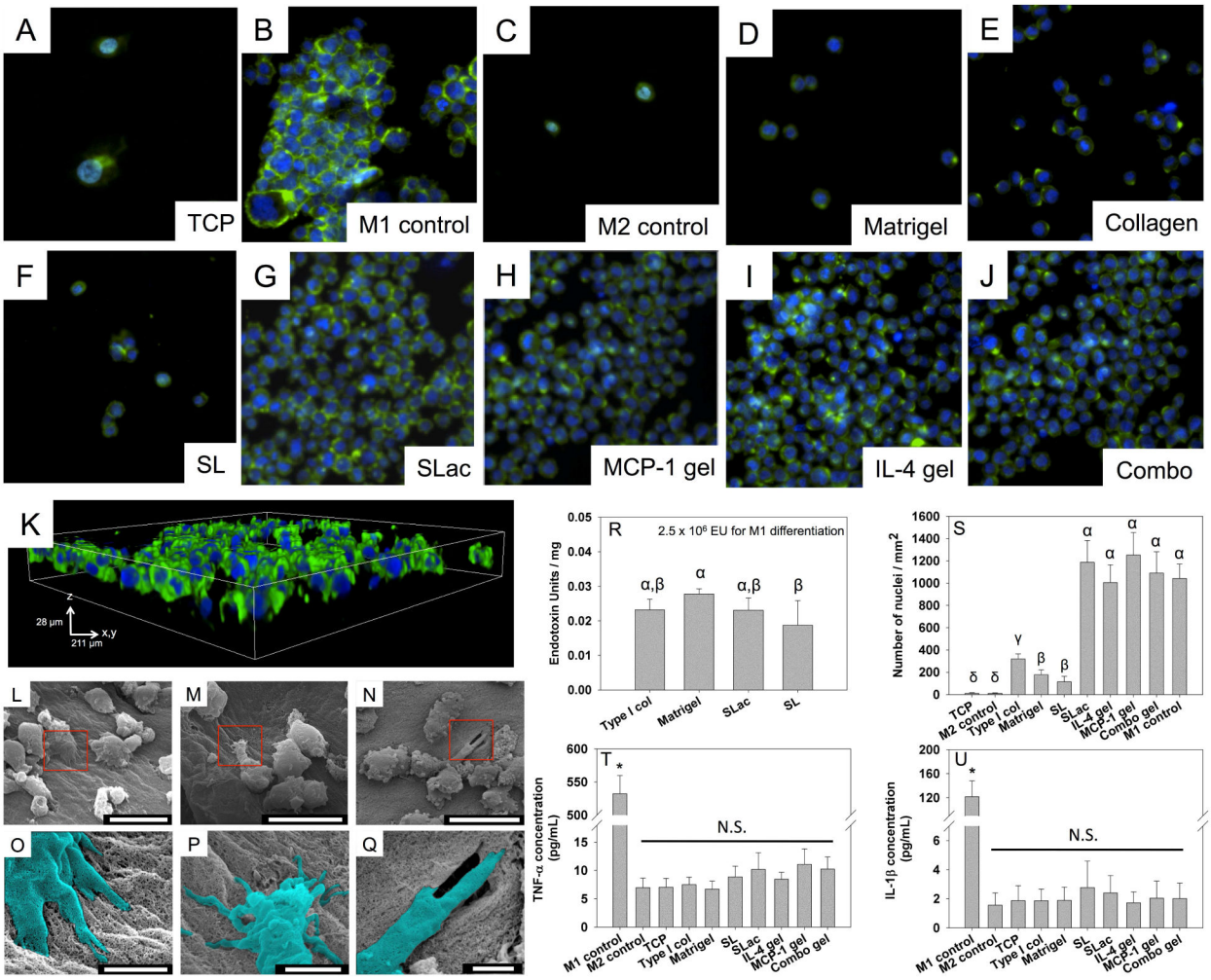

Figure 3. THP-1 cell adhesion to material surfaces

Cell incubated on TCP (A) were differentiated to M1 phenotype (B) or M2 phenotype (C). Matrigel (D), Collagen (E) and SL (F) did not show as high cell adhesion, compared to SLac (G), with MCP-1 (H) or IL-4 (I) or both (J). THP-1 cells grown on SLac show infiltration into hydrogels (K) at 3 days. Scale: A-J are 237µm wide, K is 211 µm square base x 28 µm height. SEM images show cell adhesion to nanofibrous surface (L), extending filapodia into peptide matrix (M), and potentially degrading/remodeling matrix (N). Cell-matrix interactions more clearly seen in magnified false colored images of regions in red boxes (L–O, M–P, N–Q). Scale bar L–M: 20µm, O–Q: 3µm. Endotoxin content of MDP scaffolds was not significantly different compared to commercially available materials (R), but showed significantly higher THP-1 cell adhesion (S) when –RGDS moiety was present: SLac, IL-4 gel, MCP-1 gel and combo gel. Media aliquots from THP-1 cells incubated on scaffolds did not show a significant increase in pro-inflammatory cytokine release of TNF-α (T) or IL-1β (U). Similar Greek letter indicate no statistically significant difference ($p<0.01$).

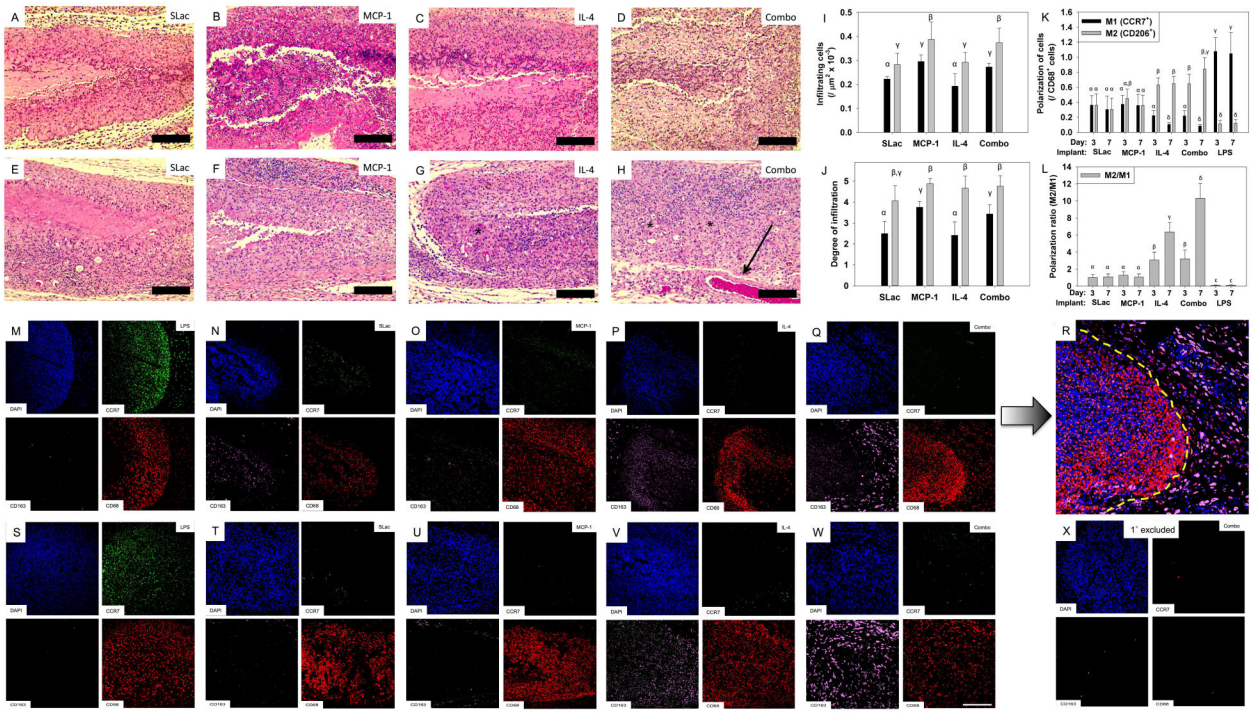

Figure 4. Characterization of cellular infiltrate

H&E staining for infiltrating cells into SLac, MCP-1, IL-4 or Combo scaffolds, 3 day: A,B,C,D and 1 week: E, F, G, H, respectively. At early timepoints (3 day) cells can be seen infiltrating the implants with greatest infiltration in MCP-1 implants. All scaffolds show an increase in cellular infiltrate at the 7 day time points (I) and infiltration into the center of the scaffold (J), grey bar 3 day, black bar 7 day. Immunostaining to determine macrophage polarization at 3 day: M–R and 1 week: S–W. Majority of DAPI stained cells co-stain for macrophage marker CD68. LPS loaded scaffolds stain positive for CCR7 (M1 marker) and scaffolds loaded with IL-4 show increased staining for CD163 (M2 marker). (R) Composite image (of Q) showing influence of released cytokines (MCP-1 and IL-4) from scaffold (left of dotted yellow line) on recruitment and M2 polarization of macrophages in the vicinity of the implant (right of dotted yellow line). (K) Quantification of macrophage polarization showing increase in M2 polarization over time for IL-4 and combo scaffolds, (L). (X) Control: primary antibodies omitted. Full size images shown in Supplementary Figures 8–14. Similar Greek letter indicate no statistically significant difference ($p<0.01$). Scale bar: 200μm.